thesis

Ing. Ramia Deeb

Thermal Calculations of Permanent Magnet Motors in High Current Technology

BRNO UNIVERSITY OF TECHNOLOGY

FACULTY OF ELECTRICAL ENGINEERING AND COMMUNICATION

DEPARTMENT OF POWER ELECTRICAL
AND ELECTRONIC ENGINEERING

CENTRE FOR RESEARCH
AND UTILIZATION OF RENEWABLE ENERGY

Ing. Ramia Deeb

THERMAL CALCULATIONS OF PERMANENT
MAGNET MOTORS IN HIGH CURRENT TECHNOLOGY

TEPELNÉ VÝPOČTY MOTORŮ S PERMANENTNÍMI MAGNETY
V SILNOPROUDÉ ELEKTROTECHNICE

Short Version of Ph.D. Thesis

Study Field:	Power Electrical and Electronic Engineering
Supervisor:	Prof. RNDr. Vladimír Aubrecht, CSc.
Opponents:	Doc. Ing. Vladislav Singule, CSc.
	Ing. Jiří Duroň, Ph.D
Defending date:	15. 11 2013

Keywords

Permanent magnets, PM machine, Joule losses, eddy current losses, FEMM, ANSYS, ANSOFT, heat, CFD, fluid flow, radial fan, cooling.

Klíčová slova

Permanentní magnety, stroj s permanentními magnety, joulové ztráty, ztráty vířivými proudy, FEMM, ANSYS, ANSOFT, teplo, CFD, proudění, radiální ventilátor, chlazení.

The dissertation thesis is at one's disposal:
Vědecké oddělení FEKT VUT v Brně, Technická 3058/10, 616 00 Brno

Contents

1 INTRODUCTION

Applying of permanent magnet materials to the electrical machines causes a big industrial revolution, because of improvement of their efficiency by eliminating the excitation losses. The air gap magnetic flux density increases, which means greater output power for the same main dimensions. The applications of PM motors have been significantly increased in spite of the high cost of permanent magnet materials.

This thesis focuses on the permanent magnet synchronous machine designed with a surface magnet rotor. The main objective of this work is to deal with a cooling system of the servo motor, since the effective cooling is very important for low speed permanent magnet (PM) machines due to their high power density and low speed.

This thesis deals with the following tasks:
- Modelling of the M 718 I servo motor
- Thermal analysis
- Magnetic analysis
- Determination of servo motor losses
- Design of cooling system
- Proposal of modifications of the servo motor model
- Thermal and magnetic analysis of the modified model
- Comparison of the results between the original and the modified motor models
- Measurements
- Results evaluation

In this thesis, modern software tools are used. These programs offer solutions for magnetic, thermal, and fluid flow problems with satisfied results without enormous demands on computing time and with no need of geometry simplifications.

2   MOTOR DESCRIPTION

The analysed M 718 I servo motor is produced by VUES Brno company. It is built with a surface magnet rotor. Such motor can be used as a part of a system, where industrial automation exists: for example, production of automobiles, robots, food industry, and glass bottles, etc.

Parameters of the M 718 I servo motor are as follows:

Voltage	280 V
Current	11.56 A
Torque	16.5 Nm
Speed	3000 rpm
Output power	5174 W
Number of poles	6

Classification of M 718 I servo motor:

- Stator: designed of 18 slots
    - Dimensions:
        - The outer diameter: 126 mm
        - The inner diameter: 63 mm
        - Length: 225 mm
- Solid rotor with PMs mounted on its surface
    - Dimensions:
        - The outer diameter: 61.6 mm
        - The inner diameter: 30 mm
- Permanent magnets:
    - Amount: 9
    - Length: 25 mm
    - Height: 3.5 mm
    - Width: 14 mm
    - Weight: 1.05 kg
- Air gap
    - Width: 0.7 mm
- Coils
    - Insulation class F
    - Pure wire weight 4.5 kg

Permanent magnets of NdFeB type are applied to the analysed servo motor. This material belongs to the rare earth magnet. The main properties of this material are high remanent magnetic flux density, high coercive force, high energy product, linear demagnetization curve.

The real servo motor and its cross-section are presented as follows:

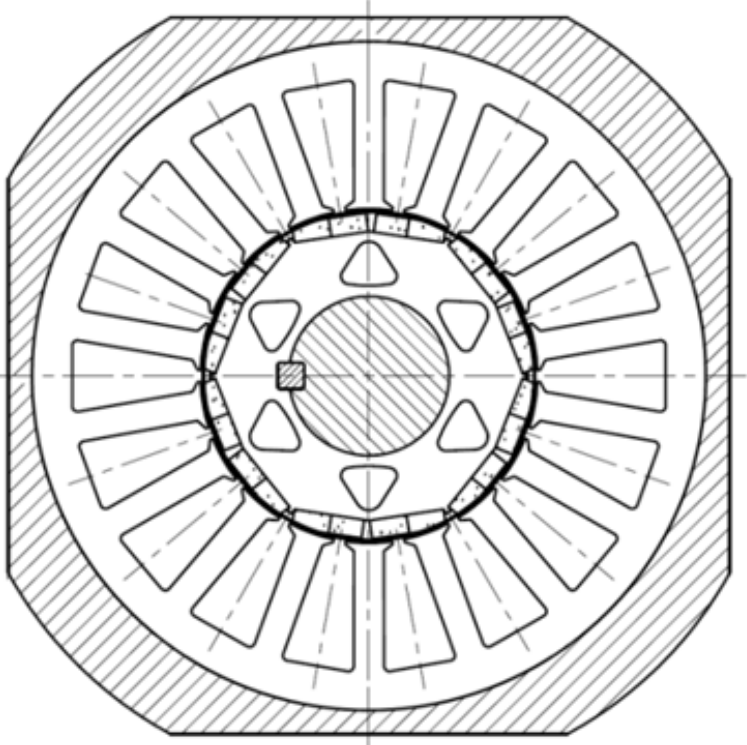
Fig. 2.1: Real M 718 I servo motor [38].

Fig. 2.2: Cross-section of M 718 I servo motor [38].

3 ANALYSIS OF MAGNETIC FIELD OF THE M 718 I SERVO MOTOR

In this thesis, the magnetic field of M 718 I servo motor is computed both 2-dimensionally (2D) and 3-dimensionally (3D). The magnetic field is calculated by the method of finite elements (FEM). Distribution of the magnetic flux density and lines along a cross-section of the servo motor is presented. Distribution curve of air-gap flux density is also presented.

3.1 2D MAGNETIC ANALYSIS

2D magnetic analysis is computed using FEMM software. The magnetic analysis is performed for the case of nominal current $I_n = 11.56$ A is applied to the servo motor armature winding.

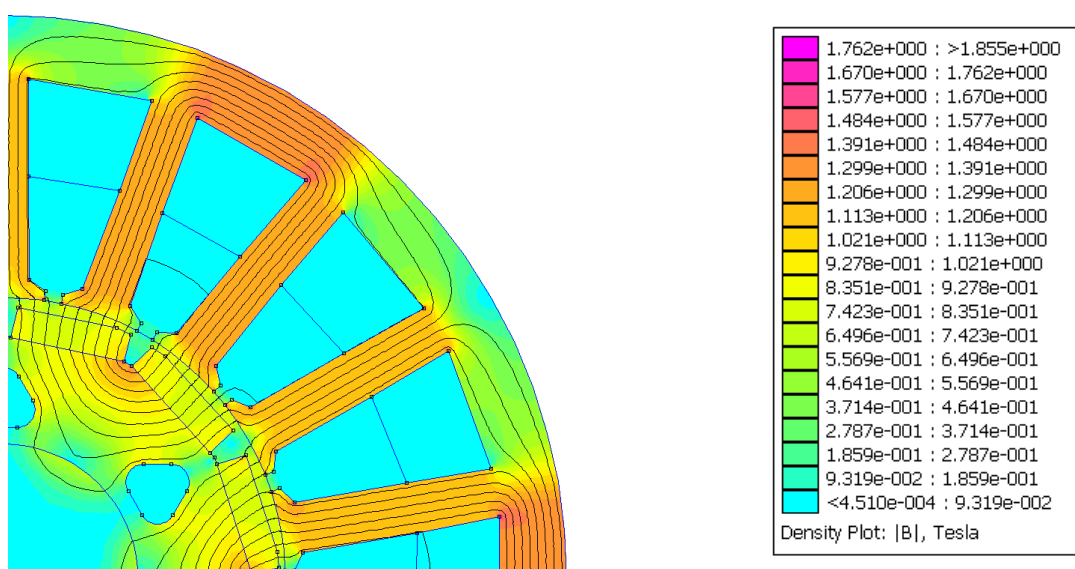|	
	1.762e+000 : >1.855e+000
	1.670e+000 : 1.762e+000
	1.577e+000 : 1.670e+000
	1.484e+000 : 1.577e+000
	1.391e+000 : 1.484e+000
	1.299e+000 : 1.391e+000
	1.206e+000 : 1.299e+000
	1.113e+000 : 1.206e+000
	1.021e+000 : 1.113e+000
	9.278e-001 : 1.021e+000
	8.351e-001 : 9.278e-001
	7.423e-001 : 8.351e-001
	6.496e-001 : 7.423e-001
	5.569e-001 : 6.496e-001
	4.641e-001 : 5.569e-001
	3.714e-001 : 4.641e-001
	2.787e-001 : 3.714e-001
	1.859e-001 : 2.787e-001
	9.319e-002 : 1.859e-001
	<4.510e-004 : 9.319e-002

Density Plot: |B|, Tesla

Fig. 3.1: Distribution of both magnetic flux density and lines inside the M 718 I servo motor.

On load, the circumferential distribution of the air-gap flux density in permanent magnet synchronous machine has a distorted waveform caused by the saturation effect on the rotor. The results of the magnetic flux density distribution in the air-gap between stator and rotor are presented in Fig. 3.2.
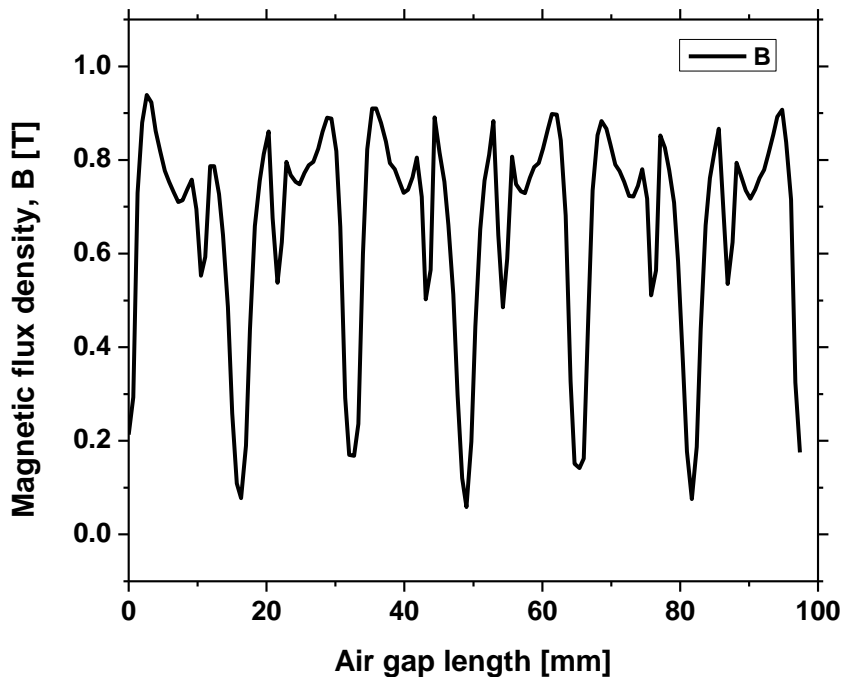
Fig. 3.2: Circumferential distribution of the magnetic flux density in the air-gap centre in the 2D analysis.

From Fig. 3.2, it can be noted that the distribution of the magnetic field is irregular because of the fractional-slot winding structure. The magnetic field increased in some air-gap parts and decreased in other parts.

3.2 3D MAGNETIC ANALYSIS

3D magnetic analysis of the M 718 I servo motor is computed using Maxwell 3D program (ANSOFT). The magnetic analysis is computed in the case of nominal current I_n applied to the armature winding. 3D model of the analysed motor is generated using RMxpert program. The computational results of the 3D magnetic analysis are presented in the following figure.
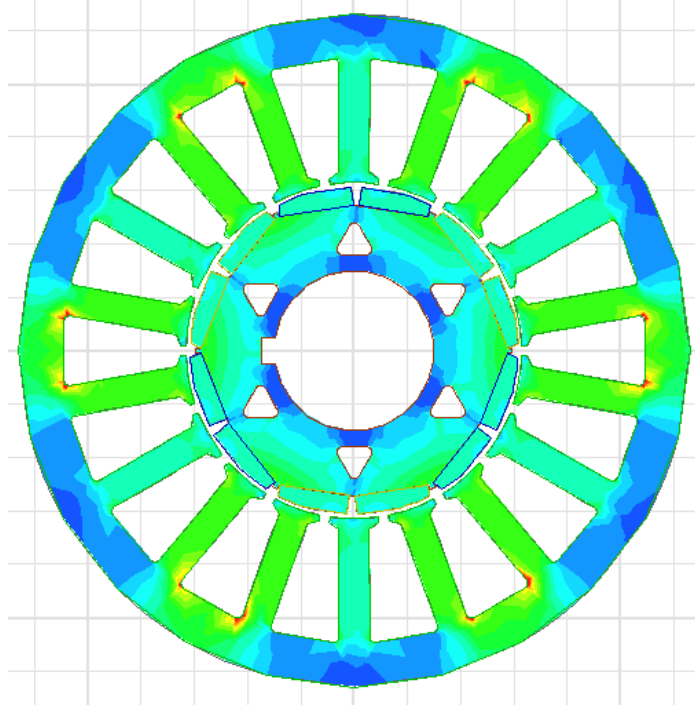

Fig. 3.3: Distribution of magnetic flux density along a cross-section of the servo motor.

Fig. 3.3 presents the distribution of the magnetic flux density along a cross-section of the servo motor. The interaction between the magnetic field produced by the stator winding and the magnetic field produced by the permanent magnets can be shown clearly.

4 LOSSES CALCULATION

Losses in an electrical machine can be classified into copper losses, core losses and rotor losses. Joule losses and eddy current losses are calculated for the M 718 I servo motor.

4.1 JOULE LOSSES

Ohmic losses are calculated using Maxwell 3D program. Eddy current solver is used for this purpose. Distribution of the ohmic losses in the stator windings is presented as follows:
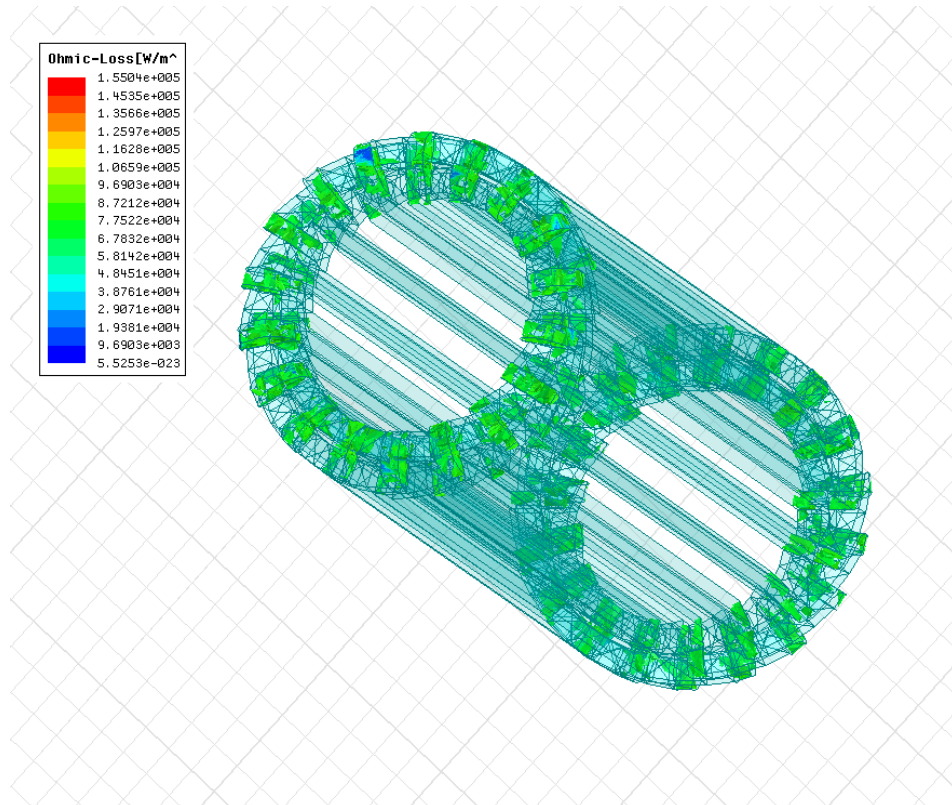

Fig. 4.1: Distribution of ohmic losses in the stator windings.

The calculated value of the Joule losses is about $\Delta P_{Joule} = 100.8$ W.

4.2 EDDY CURRENT LOSSES

Eddy current losses are generated in the permanent magnets due to the time-harmonics by non-sinusoidal input waveform and to the space-harmonics by non-constant reluctance because of stator slotting. These losses may cause significant heating of the permanent magnets, due to the relatively poor heat dissipation from the rotor, and result in partial irreversible demagnetization, particularly of NdFeB magnets, which have relatively high temperature coefficients.

The relationship used for calculation of the eddy current losses in the magnets is presented as follows [19]:

$$P_m \approx \frac{V_m b_m{}^2 \hat{B}_m{}^2 \omega^2}{12 \rho_m} \ ,$$

4.1

where:

ω frequency
V_m magnet volume
b_m magnet width
ρ_m magnet resistivity
B magnetic flux density in the air-gap.

Calculation results

The calculation results of eddy current losses are presented for both 2D and 3D analyses.

For 2D analysis $\Delta P_{eddy} = 48$ W.
For 3D analysis $\Delta P_{eddy} = 54$ W.

5 DESIGN OF SERVO MOTOR COOLING SYSTEM

The flow process in an electrical machine is highly complicated and it cannot be well described with the older methods. Measurements inside a fast rotating rotor are very complicated due to the high circumferential speed. The 3D computational fluid dynamics (CFD) is the best alternative for this analysis; thereby the flow properties can be calculated without geometry simplification, in addition to couple thermal and flow calculations using dedicated programs. Two cooling models are designed for the analysed M 718 I servo motor (internal and external).

5.1 FLUID FLOW MODEL

The flow of an incompressible fluid can be described according to the Reynolds averaged Navier-Stokes equations as follows [33, 34]:

$$\rho \frac{\partial U}{\partial t} - \eta \nabla \cdot \nabla U + \rho U \cdot \nabla U + \nabla P + \nabla \overline{(\rho u' \otimes u')} = F$$

$$\nabla \cdot U = 0$$

(5.1)

where:

η dynamic viscosity
U vector velocity
ρ fluid density
P pressure
F vector of volumetric force

The last term in the left hand of the above equation (dyadic operator) is called the Reynolds stress tensor. It describes the fluctuations around a mean flow. The $\kappa\text{-}\varepsilon$ model is used for this analysis. This model is based on the following equations:

$$\rho \frac{\partial U}{\partial t} - \nabla \cdot \left[\left(\eta + \rho C_\mu \frac{\kappa^2}{\varepsilon} \right) \cdot \left(\nabla U + \left(\nabla U \right)^T \right) \right] + \rho U \cdot \nabla U + \nabla P = F$$

$$\nabla \cdot U = 0$$

(5.2)

where:
κ turbulent kinetic energy
ε dissipation rate of the turbulent energy

The k, ε variables introduce the following equations:

$$\rho \frac{\partial \kappa}{\partial t} - \nabla \cdot \left[\left(\eta + \rho \frac{C_\mu}{\sigma_\kappa} \frac{\kappa^2}{\varepsilon} \right) \nabla \kappa \right] + \rho U \cdot \nabla \kappa = \rho C_\mu \frac{\kappa^2}{2\varepsilon} \left(\nabla U + (\nabla U)^T \right)^2 - \rho \varepsilon$$

$$\rho \frac{\partial \varepsilon}{\partial t} - \nabla \cdot \left[\left(\eta + \rho \frac{C_\mu}{\sigma_\varepsilon} \frac{\kappa^2}{\varepsilon} \right) \nabla \varepsilon \right] + \rho U \cdot \nabla \varepsilon = \rho C_{\varepsilon 1} \frac{\kappa}{2} \left(\nabla U + (\nabla U)^T \right)^2 - \rho C_{\varepsilon 2} \frac{\varepsilon^2}{\kappa} \tag{5.3}$$

where:

$C_\mu, C_{\varepsilon 1}, C_{\varepsilon 2}, \sigma_\kappa, \sigma_\varepsilon$ model constants

5.2 TRANSIENT THERMAL MODEL

A 3D transient thermal analysis is computed using ANSYS Workbench software. The fluid parameters such as the heat transfer coefficients of convection are taken from the 3D turbulent model. These parameters represent the input of the transient thermal analysis. The conditions on the solid wall that is in a contact with the cooling fluid (air) are modelled using the boundary condition for the heat flux q as follows [33, 34]:

$$-n \cdot q = h(T_f - T) + q_0, \tag{5.4}$$

where:

h heat transfer coefficient of convection
T_f the temperature of the fluid close to the solid wall
q_0 heat sources on the solid surface (losses)

5.3 INTERNAL COOLING DESIGN

For this cooling type, some modifications are added to the original servo motor model:

- Cooling openings are designed in the motor frame.
- Radial fan is mounted on the motor shaft inside the frame.

The performed cooling system works as follows:

Ambient air enters inside the motor through the frame openings, passes over the heated motor parts and leaves out the motor by the fan. The fluid flow and transient thermal analyses of both original motor and modified one are computed within this work. A comparison of analysis results is performed.
The turbulent properties of the flow are modelled for 3D coupled CFD and transient thermal analysis. The flow turbulent model is performed using CFX program.
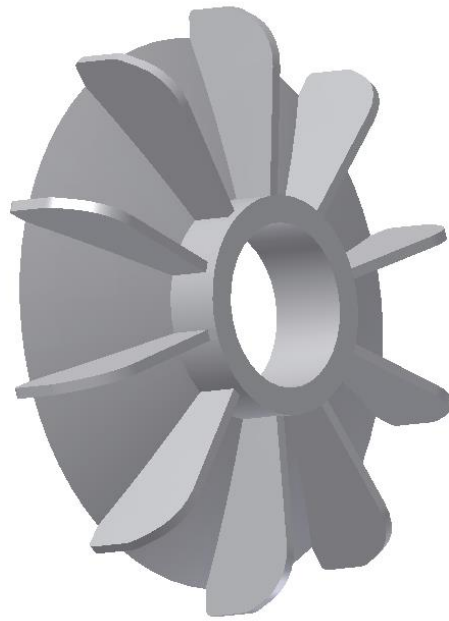
Fig. 5.1: Radial fan.

The fluid flow computational results of the modified servo motor (servo motor after adding internal cooling) are presented as follows:
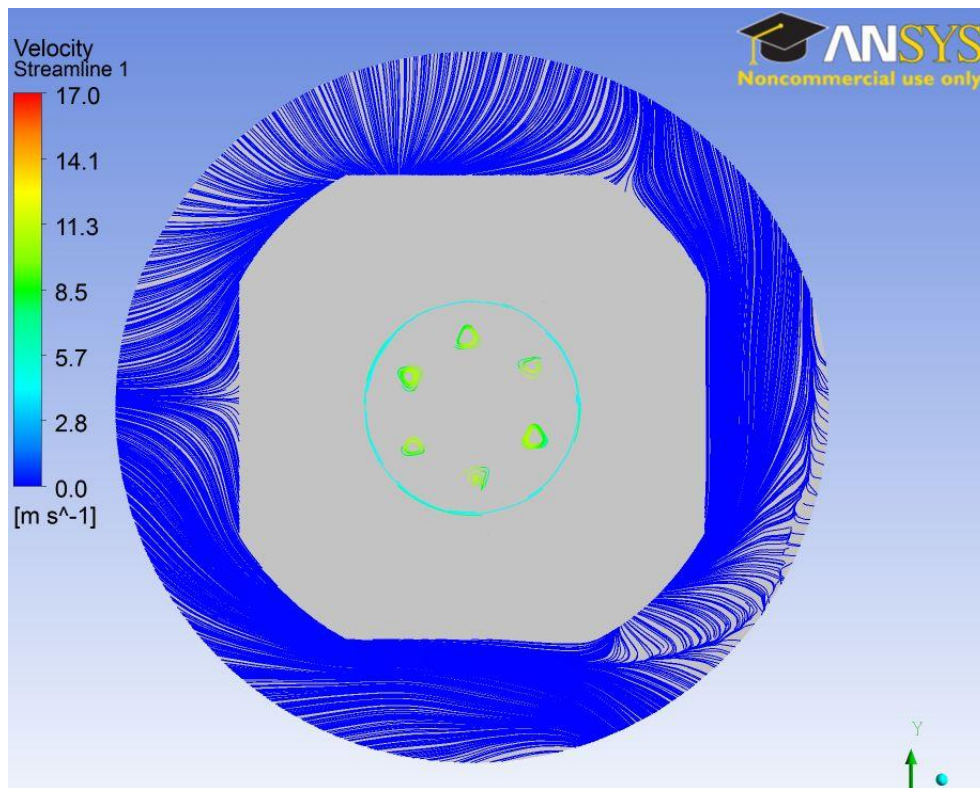

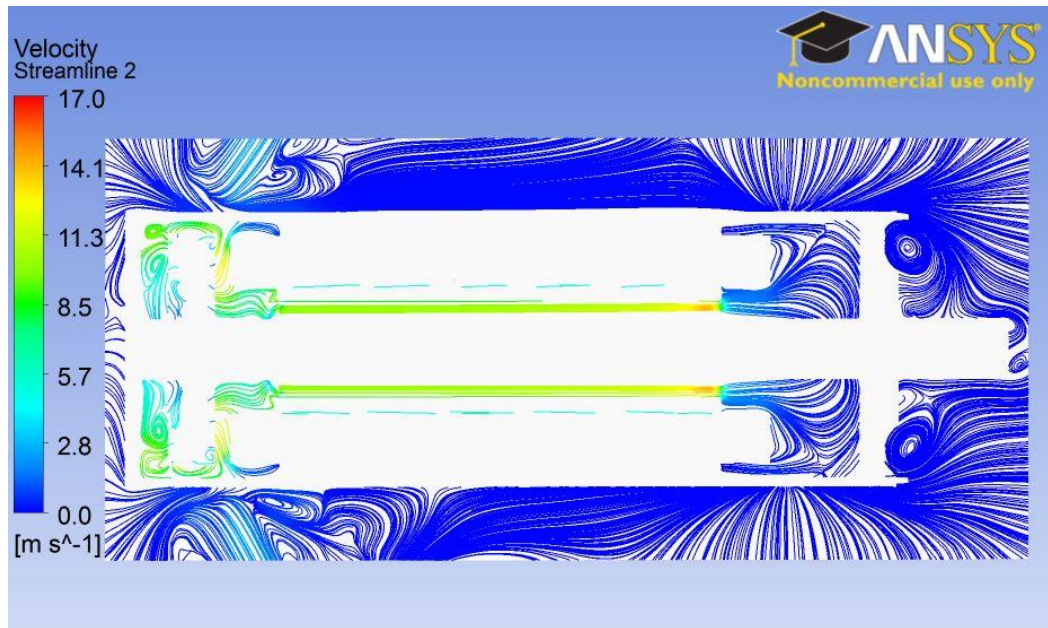Fig. 5.2: Velocity streamlines along a cross-section of the modified model of the servo motor.

Fig. 5.3: Velocity streamlines along a longitudinal-section of the modified model of the servo motor.

Fluid flow computational results of the modified servo motor can be clearly seen on both cross and longitudinal sections of the servo motor presented above. Ambient air enters inside the motor through the frame openings; air also flows through the air gap between stator and rotor and through the cooling channels on rotor. Fluid flow velocity is of about 2.8 - 17 m/s.

Transient thermal analysis of the modified motor was also computed. The temperature field distribution in the servo motor solids for both original M 718 I motor (totally closed), and modified one (internal cooled model) is presented as follows:
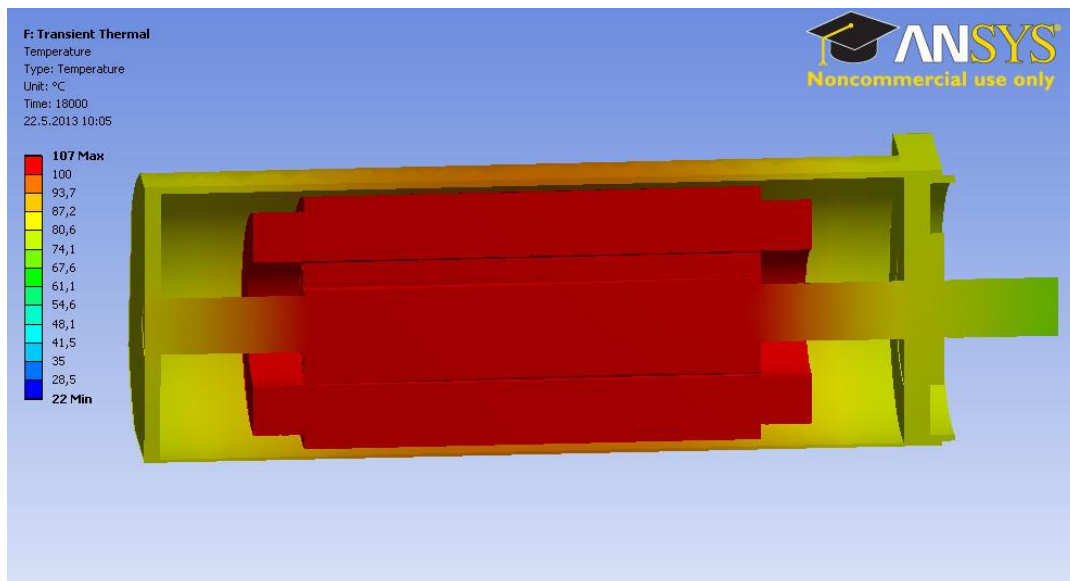

Fig. 5.4: Distribution of temperature field in the original model of the servo motor.

The maximum temperature for the original servo motor is about 107 °C. The computational results of the internal cooled servo motor are presented in the following figure.
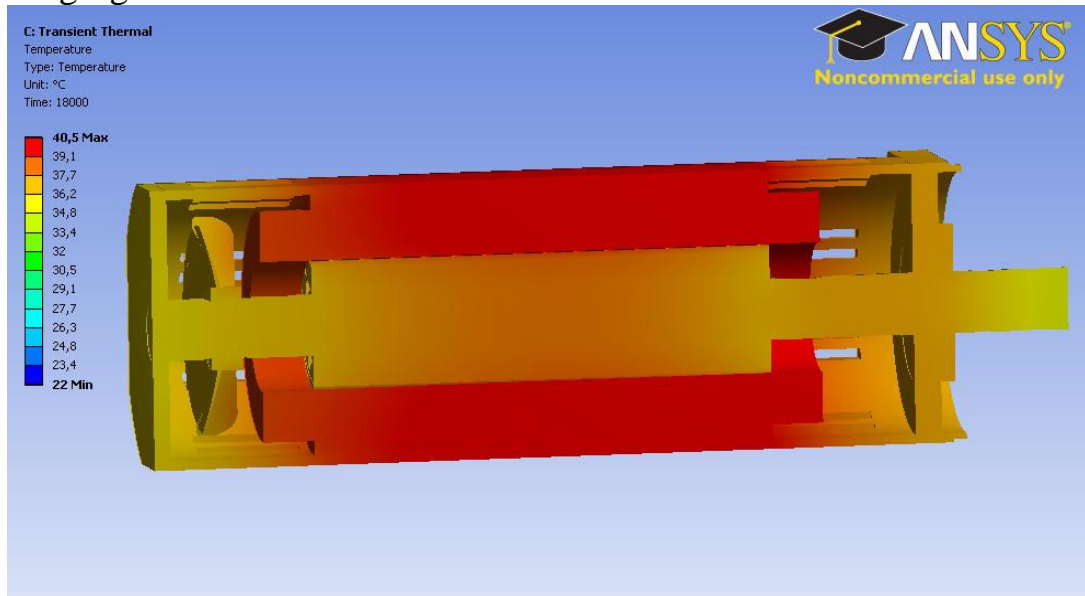

Fig. 5.5: Distribution of temperature field in the modified model of the servo motor.

Adding an internal cooling system to the original servo motor decreases its temperature to about 40.5 °C.

5.4 EXTERNAL COOLING DESIGN

5.4.1 Introduction

Heat can be transferred from the surface of a body into the surrounding space by conduction, convection and radiation, respectively. Net heat radiation occurs only when the heated body is located in the vacuum. The heat transfer by conduction in gases (e.g. air) is usually too small and it can be neglected. The convection is conditioned by heating of the air coming into contact with the heated surface of the electrical machine and by its movement. The heated air is replaced by the cold one, which is heated again and flows further. Heat transfer by convection is significantly increased by the forced circulating flow of the cooling air (artificial blowing of the heated surface). In practice, simplified formulas are usually used for the calculation of the temperature rise of electrical machines, which give the temperature gradient between the heated surface and the cooling gas. These relationships consider all kinds of heat transfer that could happen during cooling of electrical machines [35].
The temperature gradient at the surface is determined by the following relationship:

$$\Delta\vartheta_{surface} = \frac{P_{surface}}{\alpha_{surface} S_{surface}}, \tag{5.5}$$

where

$P_{surface}$ surface heat flux

$S_{surface}$ area of the cooling surface

$\alpha_{surface}$ heat transfer coefficient of the surface, which depends on a material, surface conditions, air speed along the surface, and other factors.

To improve cooling of the machines with IP 44 and IP 55 degree of protection, outer surface of the stator is equipped with cooling slots. These slots are positioned in the direction of expected movement of the cooling ambient air.
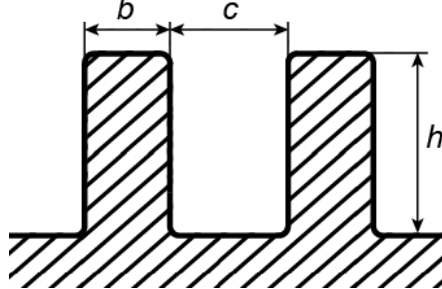

Fig. 5.6: Cooling slots on the motor frame with IP 44 and IP 55 degree of protection and with external cooling [35].

Where:

b slot thickness

c distance between slots

h slot height

Heat flux from the slotted surface of the motor frame, is composed of parts, which removes heat from the surface frame S_s corresponding to the distance c between the cooling slots (Fig. 5.6), and from the parts which dissipates heat from the slots surface S_{slots}.

$$P = (\alpha_{frame} S_{frame} + \alpha_{slots} S_{slots})\Delta\vartheta, \tag{5.6}$$

where:

α_{frame} heat transfer coefficient of slotless frame [W/m^2·K]

α_{slots} heat transfer coefficient of cooling slots, expressed on the surface of the cylindrical part of the frame with frame heating $\Delta\vartheta$ above the ambient temperature.

Adding slots to the motor frame is very effective factor for improving of the machine cooling. However, heat transfer does not grow in proportion to the slots number and their size [35].

For this cooling type some modifications are added to the original servo motor model:

- Cooling slots are designed on the original frame
- Radial fan is mounted on the motor shaft out of the frame

Fig. 5.7: Radial fan.

Fig. 5.8: Modified servo motor with external cooling.

5.4.2 Fluid flow model

A 3D flow turbulent analysis is computed using CFX software. In this analysis, solid and fluid domains are created from the motor parts and the surrounding air. The initial values of pressure, temperature and fluid velocity are applied. The computational results of the fluid flow are presented in Fig. 5.9.
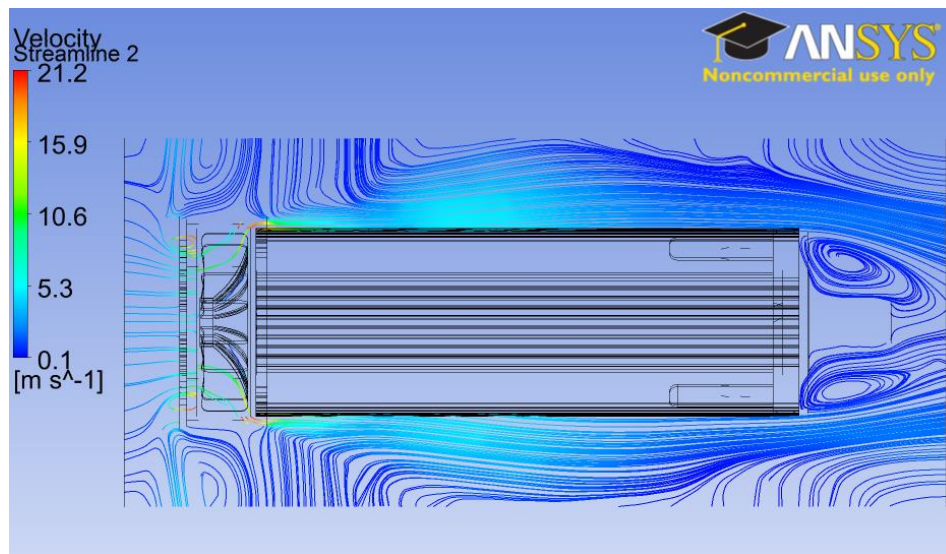

Fig. 5.9: Velocity streamlines along a longitudinal-section of the servo motor with external cooling.

From Fig. 5.9, it can be noticed that fan forces the outside air strongly inside the cooling slots on the motor surface. The air velocity is in the range of 5 m/s at the motor surface.

5.4.3 Transient thermal model

A 3D transient thermal analysis is computed using ANSYS Workbench software. The fluid parameters such as the heat transfer coefficients of convection are taken from the 3D turbulent model. These parameters represent the input of the transient thermal analysis. The other boundary conditions such as the losses generated in different parts of the servo motor (electrical, mechanical, iron, and eddy current losses) are applied. The following figures present the computational results of the thermal transient analysis for both original and servo motor with external cooling.
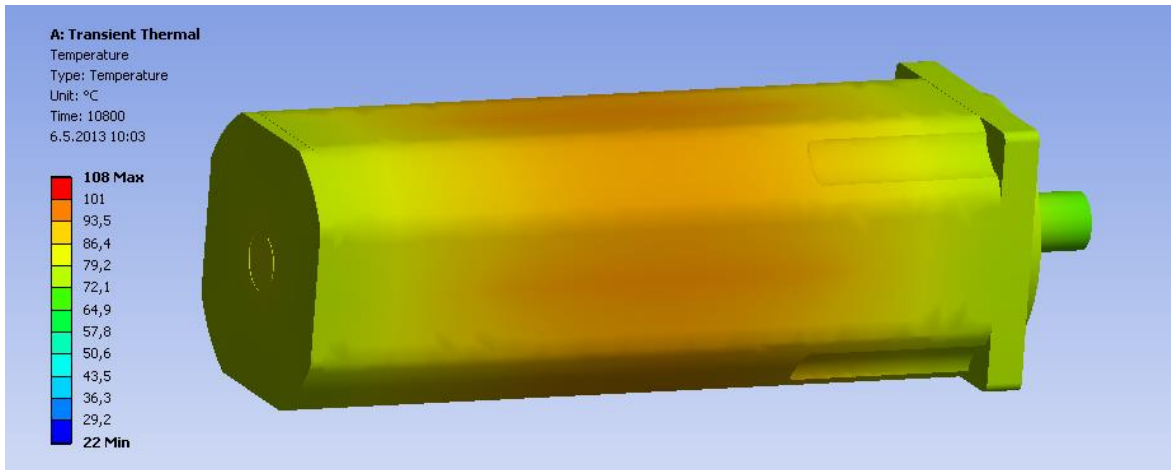

Fig. 5.10: Distribution of temperature field in the original model of the servo motor.
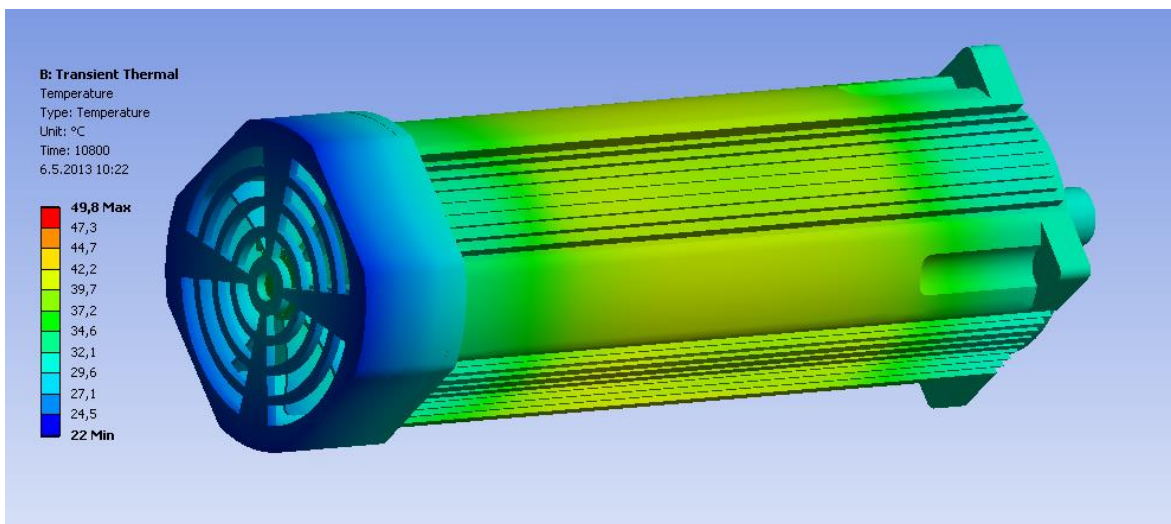

Fig. 5.11: Distribution of temperature field in the servo motor with external cooling.

The comparison of the performed results in Figs. 5.10 and 5.11 shows that adding external cooling to the original servo motor model reduces the motor temperature of 108 °C to about 50 °C.

6   MEASUREMENTS

Temperature of electrical machine can be measured in both contact and contactless methods. In contact measurement various sensors such as thermistors and thermocouples are placed directly on the machine parts. These sensors respond directly to the temperature of the surface on which they are placed. They are placed on machine surface also inside it. Since, contactless measurement is a measurement of the body surface temperature depending on the electromagnetic radiation of the wavelength 0.4 - 25 µm, sent by measured body and received by the sensor [36, 37].

The following figure presents the test room. Three sensors are placed at the servo motor surface at different places.
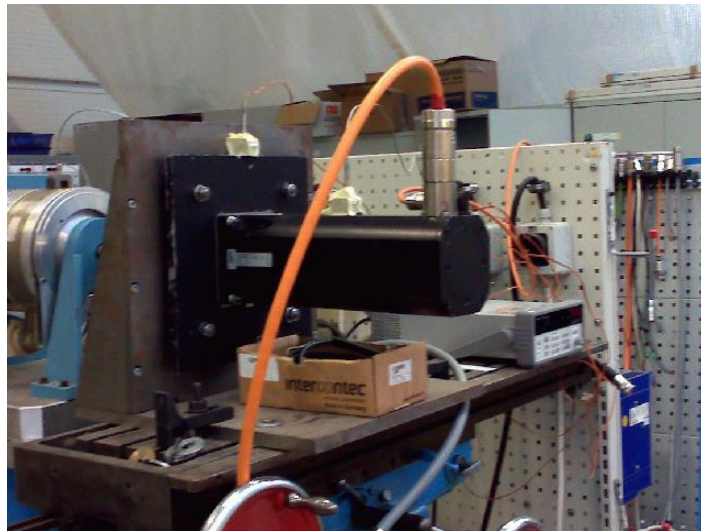

Fig. 6.1: Test room.

The results of temperature measurement using the infra-red camera are presented as follows:
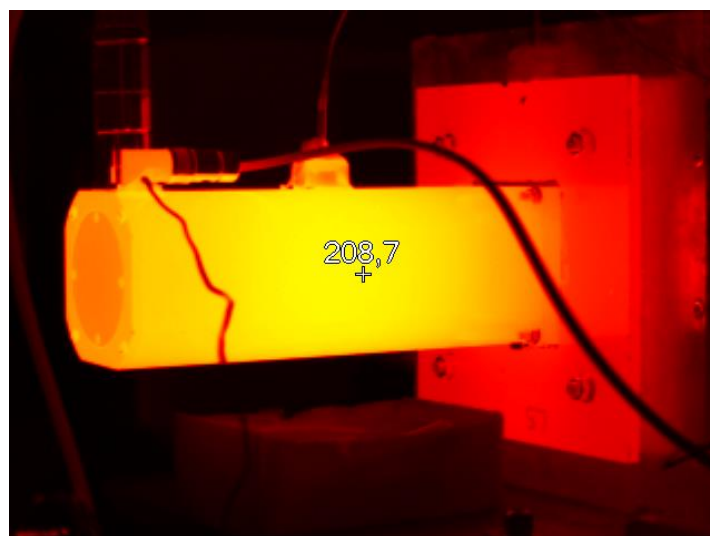

Fig. 6.2: Measured temperature using infra-red camera
(temperature is in degree of Fahrenheit).

Comparison of the computed temperature and the measured one is presented in the following figure.
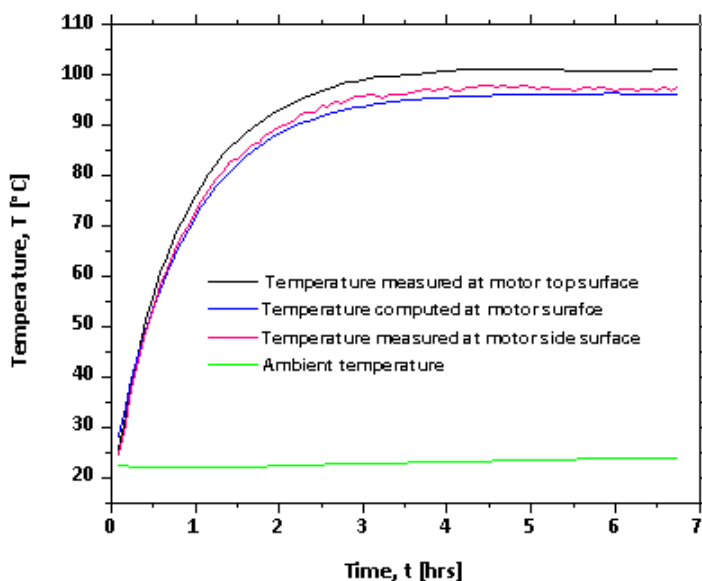

Fig. 6.3: Comparison of measured and computed temperature at surface of the servo motor.

Fig. 6.3 presents the measured temperature at different places of the servo motor surface in addition to the computed one (transient thermal analysis of the original M 718 I servo motor).

7 RESULTS AND CONCLUSION

This thesis deals with the permanent magnet servo motor of M 718 I type, produced by VUES company in Brno. The magnetic analysis of this motor is computed for both two and three dimensions. Finite element method (FEM) is used for this analysis. The computational results are presented as follows:

Tab. 7.1: Computational results of the servo motor magnetic analysis.

Magnetic analysis	B_{max} [T]	B_{PM} [T]	B_{air_gap} [T]
2D	1.76	-	0.67
3D	1.93	1.56	0.72

In this work, Joule losses are calculated using ANSOFT software, and the results are as follows:

Tab. 7.2: Comparison of measured and calculated Joule losses of the M 718 I servo motor.

Datasheet	Calculated Joule losses	Difference
102 W	100.8 W	1.2 %

Eddy current losses are calculated too and the results comparison is presented in the following table.

Tab. 7.3: Comparison of measured and calculated eddy current losses of the M 718 I servo motor.

Eddy current losses	2D	3D
Datasheet	52 W	52 W
Calculated	48 W	54 W
Difference	8 %	3.8 %

One of the other topics of the thesis is the motor cooling system. The analysed servo motor is designed as a totally enclosed motor. To improve the motor cooling system, two cooling designs are proposed (internal and external).

Tab. 7.4: Temperature of servo motor with different cooling types.

Motor type	Temperature [°C]
Original servo motor	108
Servo motor with internal cooling	40
Servo motor with external cooling	50

A comparison between the measured temperature (tested) of the servo motor and the computed one (computed using ANSYS Workbench) is presented in the following table:

Tab. 7.5: Computed and measured temperature at the servo motor surface using various methods.

Motor surface temperature		T [°C]
Computed using ANSYS Workbench		96.2
Measured using thermocouple	Surface on top	101.0
	Surface on side	97.4
Measured using infra-red camera		98.2

REFERENCES

[1] Gieras, J. F. Permanent Magnet Motor Technology, Design and Applications, Third Edition. CRC Press Taylor and Francis Group NW. 2010. ISBN: 978-1-4200-6440-7.

[2] HANSELMAN, Duane C. Brushless Permanent-Magnet Motor Design. McGraw-Hill. NW. 1994. ISBN 0-07-026025-7.

[3] Gieras, J.F.; Santini, E.; Wing, M. Calculation of synchronous reactances of small permanent-magnet alternating-current motors: comparison of analytical approach and finite element method with measurements, IEEE Transactions on Magnetics, vol.34, no.5, pp.3712-3720, Sep 1998. ISSN: 0018-9464.

[4] Chen, J.; Zhang, F. General analytical solution of magnetic field in slotted surface-mounted permanent magnet machines. International Conference on Electrical Machines and Systems (ICEMS), 2011, pp.1-6, 20-23 Aug. 2011. ISBN: 978-1-4577-1044-5.

[5] Cao, Y.; Li, Q.; Yu L. Analysis and Calculation of the Electromagnetic Field in Permanent Magnet Synchronous Motor Based on ANSYS. 1st International Conference on Information Science and Engineering (ICISE), 2009, pp.133-136, 26-28 Dec. 2009. ISBN: 978-1-4244-4909-5.

[6] Petkovska, L.; Cvetkovski, G. Hybrid analytical - FEM analysis of single phase Permanent Magnet Synchronous Motor. IEEE EUROCON '09., pp.709-716, 18-23 May 2009. ISBN: 978-1-4244-3860-0.

[7] Pinghua, T.; Guijie, Y.; Min, L.; Tiecai, L. A current control scheme with tracking mode for PMSM system. 1st International Symposium on Systems and Control in Aerospace and Astronautics, 2006. ISSCAA 2006, pp.5 pp.-876, 19-21 Jan. 2006.

[8] Zhu, Z.Q.; Ng, K., Schofield, N., Howe, D. Improved analytical modeling of rotor eddy current loss in brushless machines equipped with surface-mounted permanent magnets IEE Proceedings Electric Power Applications, vol.151, no.6, pp. 641- 650, 7 Nov. 2004. ISSN: 1350-2352.

[9] Roshen, W. Iron loss model for PM synchronous motors in transportation IEEE Conference on Vehicle Power and Propulsion, 2005, pp. 4 pp., 7-9 Sept. 2005, d. ISBN: 0-7803-9280-9.

[10] Roshen, W. Iron Loss Model for Permanent-Magnet Synchronous Motors" IEEE Transactions on Magnetics, vol.43, no.8, pp.3428-3434, Aug. 2007, doi: 10.1109/TMAG.2007.899687. ISSN: 0018-9464.

[11] Rabinovici, R.; Miller, T.J.E. Eddy-current losses of surface-mounted permanent-magnet motors. IEE Proceedings on Electric Power Applications. vol.144, no.1, pp.61-64, Jan 1997. ISSN: 1350-2352.

[12] Gieras, J.F.; Koenig, A.C.; Vanek, L.D. Calculation of eddy current losses in conductive sleeves of synchronous machines. International Conference on Electrical Machines, 2008. ICEM 2008. 18th, pp.1-4, 6-9 Sept. 2008. ISBN: 978-1-4244-1736-0.

[13] Jassal, A.; Polinder, H.; Lahaye, D.; Ferreira, J.A. Comparison of analytical and Finite Element calculation of eddy-current losses in PM machines. XIX International Conference on Electrical Machines (ICEM), 2010, pp.1-7, 6-8 Sept. 2010. ISBN: 978-1-4244-4175-4.

[14] Dunlop, W. WU. J.B., collocott, S.J. Modelling of Eddy-Current Losses in a Surface-Mounted NdFeB Permanent-Magnet Generator. Proceedings of the Seventeenth International Workshop on Rare-earth Magnets and Applications, Newark, Delaware, USA, 18-22 August 2002.

[15] Bode, C.; Canders, W. R. Advanced calculation of eddy current losses in PMSM with tooth windings. XIX International Conference on Electrical Machines (ICEM), 2010, pp.1-6, 6-8 Sept. 2010. ISBN: 978-1-4244-4175-4.

[16] Lazzari, M.; Miotto, A.; Tenconi, A.; Vaschetto, S. Analytical prediction of eddy current losses in retaining sleeves for surface mounted PM synchronous machines. XIX International Conference on Electrical Machines (ICEM), 2010, pp.1-6, 6-8 Sept. 2010. ISBN: 978-1-4244-4175-4.

[17] Seok-Hee, H.; Jahns, T.M.; Zhu, Z.Q. Analysis of Rotor Core Eddy-Current Losses in Interior Permanent-Magnet Synchronous Machines. IEEE Transactions on Industry Applications, vol.46, no.1, pp.196-205, Jan.-feb. 2010. ISSN: 0093-9994.

[18] Yunkai, H.; Jianning, D.; Jianguo, Z.; Youguang, G. Core Loss Modeling for Permanent-Magnet Motor Based on Flux Variation Locus and Finite-Element Method. IEEE Transactions on Magnetics, vol.48, no.2, pp.1023-1026, Feb. 2012. ISSN: 0018-9464.

[19] Polinder, H.; Hoeijmakers, M. J. Eddy current losses in the segmented surface mounted magnets of a PM machine. IEE Proceedings Electric Power Applications, vol.146, no.3, pp.261-266, May 1999. ISSN: 1350-2352.

[20] Hak, J., Ošlejšek, O. Cooling Calculations of Electrical Machines (in Czech). 1st part. . Physical basis for cooling and ventilation calculations. Brno. 1973.

[21] Štumberger, B.; Hadžiselimovic, M. Power and cooling capability of synchronous generator with interior per-manent magnets. Laboratory verification of machine characteristics, Przegląd Elektrotechniczny, 87 (2012). ISSN: 0033-2097.

[22] Wenming, T.; Shengnan, W.; Zhongliang, A.; Hongyang, Z.; Renyuan, T. Cooling System Design and Thermal Analysis of Multibrid Permanent Magnet Wind Generator. International Conference on Electrical and Control Engineering (ICECE), 2010, pp.3499-3502, 25-27 June 2010. ISBN: 978-1-4244-6880-5.

[23] Chong, Y. C.; Chick, J.; Mueller, M. A., Staton, D. A., McDonald, A. S. Thermal modelling of a low speed air-cooled Axial Flux Permanent Magnet generator. 6th IET International Conference on Power Electronics, Machines and Drives (PEMD 2012), pp.1-7, 27-29 March 2012. ISBN: 978-1-84919-616-1.

[24] Howey, D.A.; Holmes, A.S.; Pullen, K.R. Measure-ment and CFD Prediction of Heat Transfer in Air-Cooled Disc-Type Electrical Machines. IEEE Trans-actions on Industry Applications, vol.47, no.4, pp.1716,1723, July-Aug. 2011. ISSN: 0093-9994.

[25] Marignetti, F.; Delli Colli, V.; Coia, Y. Design of Axial Flux PM Synchronous Machines Through 3-D Coupled Electromagnetic Thermal and Fluid-Dynamical Finite-Element Analysis. IEEE Transactions on Industrial Electronics, vol.55, no.10, pp.3591,3601, Oct. 2008. ISSN: 0278-0046.

[26] Staton, D.A.; Cavagnino, A. Convection Heat Transfer and Flow Calculations Suitable for Analytical Modelling of Electric Machines. IECON 2006 - IEEE Annual Conference on Industrial Electronics, pp.4841,4846, 6-10 Nov. 2006. ISSN: 1553-572X.

[27] Howey, D.A.; Childs, P.R.N.; Holmes, A.S. Air-Gap Convection in Rotating Electrical Machines. IEEE Transactions on Industrial Electronics, vol.59, no.3, pp.1367,1375, March 2012. ISSN: 0278-0046.

[28] Bergheau, J. M., Fortunier. R. Finite Element Simulation of Heat Transfer. UK, USA: ISTE Ltd and John Wiley & Sons, Inc., 2008. ISBN 978-1-84821-053-0.

[29] Yunus A. C., Boles, M. A.: Thermodynamics- An Engineering Approach, 5th ed, McGraw-Hill, 2006, ISBN 978-0073107684.

[30] Boldea, I., Nasar, S. A. The Induction Machine Handbook. USA: CRC Press LLC, 2002. ISBN 0-8493-0004-5.

[31] Massey, B., Ward-Smith, J. Mechanics of Fluids: Eighth edition. UK: Taylor & Francis, 2006. 696 pages. ISBN 0-203-41352-0.

[32] Versteeg, H K., Malalasekera, W. An Introduction to Computational Fluid Dynamics: the finite volume method. Second Edition. England: Pearson Education Limited, 1995, 2007. ISBN 978-0-13-127498-3.

[33] Kolondzovski, Z. Numerical modelling of the coolant flow in a high-speed electrical machine. 18th Interna-tional Conference on Electrical Machines, 2008. ICEM 2008, pp.1-5, 6-9 Sept. 2008. ISBN: 978-1-4244-1736-0.

[34] Kolondzovski, Z.; Sallinen, P.; Arkkio, A. Thermal analysis of a high-speed PM machine using numerical and thermal-network method. XIX International Conference on Electrical Machines (ICEM), 2010, pp.1-6, 6-8 Sept. 2010. ISBN : 978-1-4244-4175-4.

[35] Kopylov, I. P. Design of Electrical Machines (in Czech). SNTL Praha, 1988.

[36] Webster, J. G. The measurement, Instrumentation and Sensors, CRC Press LLC, ISBN 3-540-64830-5

[37] Kreial, M. Temperature Measurement (in Czech). Praha 2005, ISBN 80-7300-145-4.

[38] Servo motor documentation- EN_M71_____070927.PDF (trade publication).

CURRICULUM VITAE

Name: Ramia Deeb
Date of birth: 2.2.1980
Place of birth: Aleppo, Syria

Education

1998 – 2003   Tishreen University, Faculty of Mechanical and Electrical engineering, Dept. of Power Engineering.
2003 – 2004   Diploma of Higher study, field of Electrical power systems, Tishreen University, Faculty of Mechanical and Electrical engineering, Dept. of Power Engineering.
2009 – 2013   Ph.D student at Brno University of Technology Dept. of Power Electrical and Electronic Engineering.

Employment

2004 – 2006   Engineer at Tishreen University, Faculty of Mechanical and Electrical engineering.
2006 – 2008   Assistant at Faculty of Mechanical and Electrical engineering, Section of Power Engineering.
2012 – 2013   Research assistant, Centre for Research and Utilization of Renewable Energy

Languages

Arabic: mother language

Czech

English

ABSTRACT

This dissertation focuses on magnetic, thermal, and cooling calculations of servo motor with permanent magnets (M718 I servo motor produced by VUES company). These calculations are achieved using dedicated software based on numerical methods of finite elements (FEM) and finite volumes (FVM).

The 2D (two dimensional) magnetic analysis of the motor is computed using FEMM (finite element method magnetics). 3D (three dimensional) magnetic analysis is computed too using ANSOFT software. From the performed analyses, distribution of the magnetic field inside the servo motor, the circumferential distribution of the magnetic flux density in the air gap centre are obtained. Eddy current losses are calculated depending on the magnets dimensions and the value of the air gap magnetic flux density. Joule losses are also calculated using ANSOFT for 3D model. Two cooling models are designed for the servo motor. In the first one, internal cooling system is used. Some modifications (openings in the motor frame and radial fan mounted on the motor shaft inside the frame) are added to the motor original model. In the second model, external cooling system is used. For this type, cooling slots are added to the original frame and radial fan is mounted on the motor shaft out of the frame. Fluid flow and thermal transient analyses are computed for the original motor and for the modified one (internal cooling and external cooling model) using ANSYS Workbench program. Heat characteristics of the original servo motor are measured using different sensors. Finally, an evaluation of the different results is performed.

ABSTRAKT

Práce se zabývá výpočty magnetických a tepelných vlastností servomotoru s permanentními magnety (motor M718 I vyráběný firmou VUES s.r.o. v Brně). Všechny uvedené výpočty jsou založené na numerických metodách konečných prvků a konečných objemů.

2D magnetická analýza motoru byla řešena s pomocí programu FEMM, zatímco pro 3D analýzu byl využit software ANSOFT. Magnetické analýzy umožnily stanovit rozložení magnetického pole v motoru a ve vzduchové mezeře. Ztráty způsobené vířivými proudy byly počítány v závislosti na rozměrech permanentních magnetů a velikosti toku magnetické indukce ve vzduchové mezeře. U 3D modelu v programu ANSOFT byly vypočítány i Joulovy ztráty. Pro daný servomotor byly navrženy dva způsoby chlazení. V prvním případě se jedná o vnitřní chladicí systém. K původnímu modelu motoru byly přidány některé modifikace (otvory v rámu motoru a radiální ventilátor na hřídeli uvnitř rámu motoru). U druhého způsobu chlazení bylo navrženo vnější chlazení. K původnímu rámu byly přidána chladicí žebra a radiální ventilátor na hřídeli vně rámu motoru. Výpočty proudění a tepelná analýza byly provedeny jak pro původní model motoru, tak i pro modifikovaný návrh (vnitřní a vnější chlazení) pomocí software ANSYS Workbench. Teplotní charakteristiky původního motoru byly měřeny různými senzory. Bylo provedeno porovnání experimentálně získaných výsledků s vypočteným teplotním modelem.